LETTER

NJC
www.rsc.org/njc

Controlled release and conversion of guest species in zeolite microcapsules

Deju Wang,†[ab] Guibo Zhu,†[a] Yahong Zhang,*[a] Wuli Yang,[c] Biyun Wu,[a] Yi Tang*[a] and Zaiku Xie[b]

[a] *Department of Chemistry, Shanghai Key Laboratory of Molecular Catalysis and Innovative Materials, Fudan University, Shanghai, 200433, P.R. China. E-mail: yitang@fudan.edu.cn; zhangyh@fudan.edu.cn; Fax: +86-21-65641740; Tel: +86-21-55664125*

[b] *Shanghai Research Institute of Petrochemical Technology, Shanghai, 201208, P.R. China*

[c] *Department of Macromolecular Science, Key Laboratory of Molecular Engineering of Polymers (Minister of Education), Fudan University, Shanghai, 200433, P.R. China*

Received (in Montpellier, France) 13th September 2004, Accepted 30th November 2004
First published as an Advance Article on the web 18th January 2005

DOI: 10.1039/b414127j

Controlled release and conversion of guest species (CO_2) in zeolite microcapsules was achieved thanks to the high microporosity and the thermal and chemical stability of the zeolite shells.

Microcapsules can encapsulate various active ingredients in their inner space, keeping them away from the surrounding environment.[1] The encapsulated species could be used to functionalize the inside of the microcapsules or could be controllably released by adjusting the encapsulator's porosity and/or the external conditions. [2,3] Up to now, a great number of microcapsules with organic polymeric shells have been successfully designed[4] and a series of useful applications for drug delivery and in the textile, petroleum, and pesticide industries has been achieved.[5] However, taking into consideration environmental compatibility and stability, an equivalent process able to encapsulate active materials into inorganic microcapsules is still desired.[1,3] Zeolite microcapsules have always been assumed to be suitable for the delivery of encapsulated guests because of their large inner volumes, stable shells and uniform micropores;[6,7] the coexistence of zeolitic shells with a variety of active guest cores (often prepared through purposeful transformation of the encapsulated species) was expected to endow them with unique catalytic and adsorption properties as microreactors.[8] In addition, because of the high thermal and chemical stability of zeolite shells, these could be more readily employed and further treated under more extreme conditions than polymer microcapsules. However, the controlled release and conversion of guest species in zeolite microcapsules remains an ongoing challenge.

Herein, by utilizing cubic or spherical $CaCO_3$ and $Fe_3(SO_4)_2(OH)_5 \cdot 2H_2O$ encapsulated zeolite microcapsules, controlled release and conversion of the encapsulated guest species inside the cavity were achieved. The target zeolite microcapsules were fabricated by hydrothermal treatment of nanosilicalite-1-seeded $CaCO_3$ or $Fe_3(SO_4)_2(OH)_5 \cdot 2H_2O$ cores in a template-free precursor gel, followed by hydrothermal treatment at 180 °C. Fig. 1 displays the SEM micrographs of the original spherical $CaCO_3$ particles [Fig. 1(A)], the zeolite-seeded spherical $CaCO_3$ cores [Fig. 1(B)] and the resulting carbonate-containing zeolite microcapsules [Fig. 1(C)]. After pre-seeding with nanosilicalite-1 and a hydrothermal treatment for a maximum of 12 h, the product retained the spherical morphology of the original $CaCO_3$ core particles and the silicalite-1 seeds originally on the $CaCO_3$ surface were converted *in situ* into dense zeolite shells built up of intergrown quadrate-shaped ZSM-5 crystals [Fig. 1(C) inset]. Additionally, using the same method with quasi-cubic $CaCO_3$ core particles, zeolite boxes encapsulating cubic $CaCO_3$ core particles were also obtained [Fig. 1(D)], whose core-shell structure could be clearly observed by TEM (Fig. 1D inset).

The micropores of MFI zeolite present in the intergrown dense zeolitic shell provide ideal nanotunnels for the controlled diffusion of small molecules or ions. Adjusting the thickness and/or the aperture of the zeolite shells should allow some control on the release of encapsulated guest species. The high acid stability of the MFI zeolite shell and the acid solubility of the $CaCO_3$ core of these samples make them a good model for such an investigation. The controlled release ability of these zeolite microcapsules was estimated by measuring the release rate of CO_2 gas from $CaCO_3$ containing zeolite microcapsules

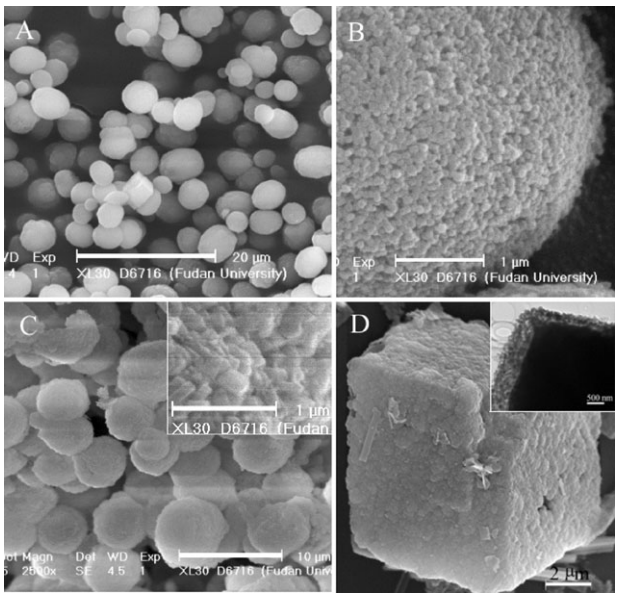

Fig. 1 SEM micrographs of the original spherical $CaCO_3$ particles (A); the surface of silicalite-1-preseeded $CaCO_3$ particles (B) and as-synthesized $CaCO_3$ containing zeolite microcapsules with spherical (C; inset: enlargement of the outer surface) and cubic (D; inset: TEM micrograph) morphologies.

† Authors contributed equally to this communication.

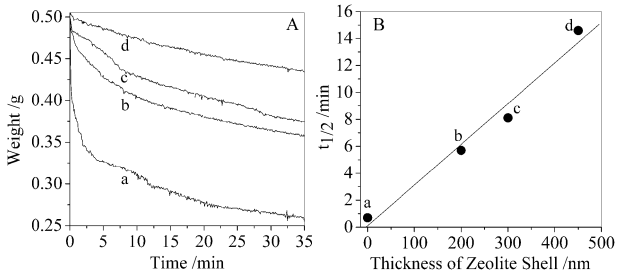

Fig. 2 (A) Time dependence of the release of CO_2 gas from bare $CaCO_3$ (curve a) and from as synthesized $CaCO_3$ containing zeolite microcapsules, after hydrothermal treatment at 180 °C for: 6 h (curve b; thickness of the resulting microcapsule ~200 nm), 9 h (curve c; thickness ~300 nm) and 12 h (curve d; thickness ~450 nm). (B) Half-life time ($t_{1/2}$) of $CaCO_3$ core dissolution *versus* the thickness of the corresponding zeolite shell. Data points a–d in Fig. 2(B) correspond to the samples giving the curves a–d in Fig. 2(A).

of various shell thicknesses (thickness control was obtained by varying the time of the hydrothermal treatment at 180 °C; see caption in Fig. 2 and Experimental). Equivalent amounts of $CaCO_3$ particles and $CaCO_3$ encapsulated microcapsule samples were added to separate 0.5 M HCl solutions (containing an excess of acid relative to the carbonate). As expected, the weight of bare $CaCO_3$ particles decreased rapidly with time [Fig. 2(A), curve a], while CO_2 release from $CaCO_3$ containing zeolite microcapsules was slower and depended on the zeolite shell thickness [Fig. 2(A), curves b–d]. Fig. 2(B) displays the relationship between the half-life time $t_{1/2}$ of encapsulated $CaCO_3$ dissolution and the shell thickness of the zeolite microcapsules, indicating that the CO_2 release rate is almost linearly proportional to the thickness of the zeolite shells. This phenomenon illustrates that zeolite shells with uniform micropores (*ca.* 0.54 nm) definitely have a limiting effect on the permeation of H_3O^+ (size *ca.* 0.37 nm) and/or CO_2 (size *ca.* 0.46 nm). Moreover, the good dependence of the release rate of CO_2 on shell thickness implies that the zeolite shells of these samples are mostly integral and homogeneous.

The X-ray diffraction (XRD) patterns of the microcapsules before and after removal of the $CaCO_3$ core (Fig. 3) indicate that the $CaCO_3$ core has been fully dissolved during the process. The flat baseline and the high-intensity MFI diffraction peaks indicate the high crystallinity of the zeolite shells. Fig. 4 presents SEM micrographs of the hollow structures after

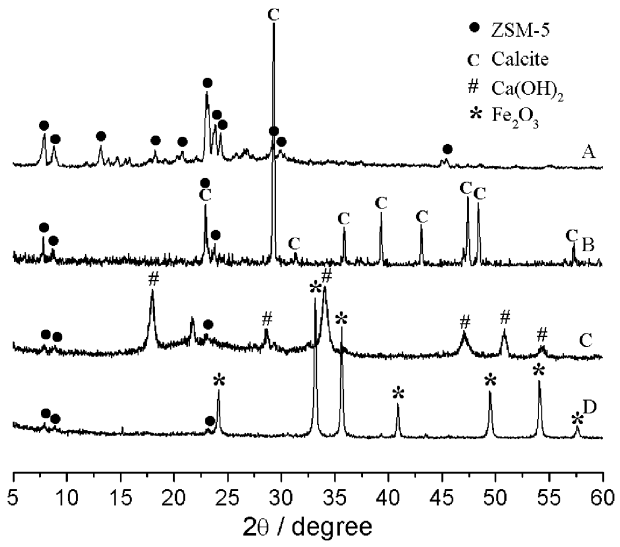

Fig. 3 XRD pattern of the zeolite microcapsules before (B) and after (A) the release of the cubic $CaCO_3$ core and after converting the core into $Ca(OH)_2$ (C) and Fe_2O_3 (D).

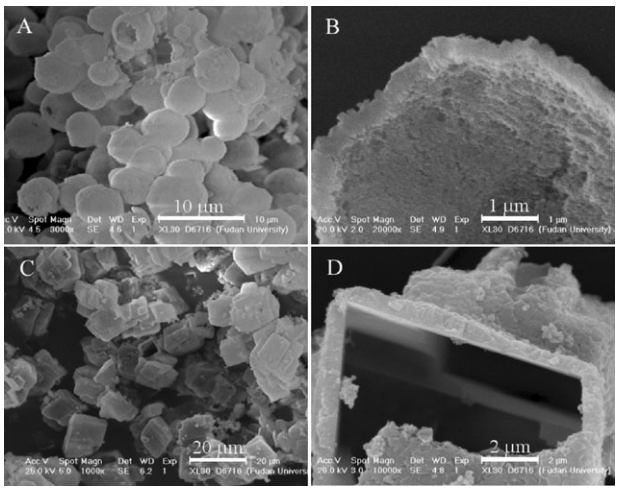

Fig. 4 SEM micrographs of (A) the hollow zeolite spheres, (B) a broken hollow zeolite sphere, (C) the hollow zeolite boxes, and (D) a broken hollow zeolite box after total release of the $CaCO_3$ core.

full dissolution of the $CaCO_3$ core, which further indicate the high acid stability and the integrality of the MFI zeolite shells.

Compared to polymer microcapsules, encapsulated guests in the cavities of zeolite microcapsules should be easily transformed into their derivatives *via* post-treatment, thus broadening the scope of their applications, thanks to the high thermal and chemical stability of zeolite shells. Fig. 5 shows the SEM and TEM micrographs of calcined spherical $CaCO_3$ and quasi-cubic $Fe_3(SO_4)_2(OH)_5 \cdot 2H_2O$ containing zeolite microcapsules. When spherical $CaCO_3$ was used as the original core, the spherical morphology was maintained after calcination at 850 °C [Fig. 5(A)], the core-shell structure being clearly observed by TEM [Fig. 5(B)]. The XRD pattern (spectrum C in Fig. 3) interestingly exhibited diffraction peaks of $Ca(OH)_2$, besides the typical ZSM-5 zeolite peaks. The formation of $Ca(OH)_2$ cores could be explained by the possible reaction of the highly hygroscopic CaO cores produced during calcination with water molecules from the atmosphere. Reconversion of the $Ca(OH)_2$ cores into $CaCO_3$ should be feasible in a CO_2 containing environment, but was not attempted. When using quasi-cubic $Fe_3(SO_4)_2(OH)_5 \cdot 2H_2O$ as the core, Fe_2O_3 encapsulated zeolite boxes were obtained after calcination at 900 °C [Fig. 5(C,D)]. Formation of Fe_2O_3 encapsulated zeolite micro-

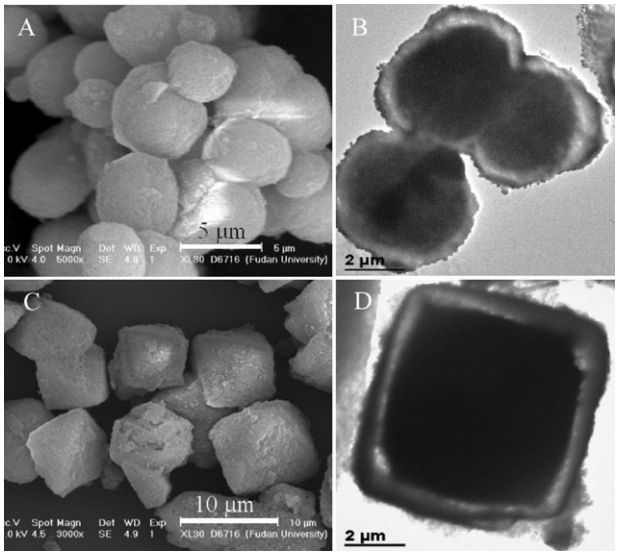

Fig. 5 SEM (A, C) and TEM (B, D) micrographs of the resulting $Ca(OH)_2$ (A, B) and Fe_2O_3 (C, D) encapsulated zeolite microcapsules after calcining zeolite microcapsules containing spherical $CaCO_3$ and quasi-cubic $Fe_3(SO_4)_2(OH)_5 \cdot 2H_2O$, respectively.

capsules was confirmed by the coexistence of Fe_2O_3 and zeolite ZSM-5 diffraction peaks in their XRD pattern (spectrum D in Fig. 3). Such microcapsule materials with tunable core species {*e.g.*, alkaline [CaO or $Ca(OH)_2$] or redox (Fe_2O_3) cores here} could be further developed to become a novel type of microreactor for catalysis and adsorption.

In summary, the controlled release of guest species encapsulated in inorganic zeolite microcapsules was achieved by controlling the thickness of microporous zeolite shells. Moreover, because of the high thermal and chemical stability of zeolite shells, the cores in the zeolite microcapsules could be easily converted into their derivatives through thermal post-treatments. These microcapsules with a zeolitic shell are expected to be promising encapsulators for guest delivery. Based on the synergistic effects of zeolitic shells and their encapsulated active species, functionalized zeolitic microcapsules could be developed as novel microreactors.

Experimental

Preparation of core particles and silicalite-1 nanocrystals

$CaCO_3$ particles with cubic and spherical morphologies were synthesized according to the literature.[9] XRD analysis of the as-synthesized $CaCO_3$ particles confirmed that both $CaCO_3$ particles are crystalline (curve B in Fig. 3): the spherical ones are mixed crystals of calcite and vaterite, while the cubic ones are pure calcite crystals.

$Fe_3(SO_4)_2(OH)_5 \cdot 2H_2O$ particles were produced by hydrothermal treatment of $Fe_2(SO_4)_3$ and urea solution mixtures. Typically, 18.25 g of $Fe(NO_3)_3 \cdot 9H_2O$, 8.91 g of $(NH_4)_2SO_4$ and 1 g of urea were added to 250 ml of water and stirred, then the mixture was put into a Teflon-coated autoclave at 150 °C for 3 h.

Silicalite-1 nanocrystals (80 ± 10 nm) were synthesized according to the literature.[10] The mean diameter of the silicalite-1 particles was *ca.* 80 nm, as measured from SEM micrographs.

Fabrication of zeolite microcapsules

The core particles (~0.1 g) were first modified by a three-layer polyelectrolyte film (PDDA/PSS/PDDA) [PDDA: poly (diallyldimethylammonium chloride); PSS: poly(sodium 4-styrene sulfonate)],[6] which provided core particles with a positively charged outer surface. Then, the negatively charged silicalite-1 nanocrystals were deposited onto the polyelectrolyte-modified core particles through electrostatic interactions. Unbound zeolite seeds were removed by washing with 0.01 M NH_4OH and centrifugation. Afterwards, the seed-coated core particles were dispersed in 2.0 ml of a solution containing a template-free gel with the composition $28\,Na_2O : 1.5\,Al_2O_3 : 100\,SiO_2 : 4000\,H_2O$ (molar ratio) in a Teflon-lined autoclave.[11] The autoclave was closed and heated in an oven at 180 °C for different periods of time (6–12 h).

Controlled release test of zeolite microcapsules

25 mL of 0.5 M HCl were put in a beaker and placed on an electronic balance. 0.5 g of $CaCO_3$ containing zeolite microcapsules was poured into the above HCl solution to dissolve the $CaCO_3$ core. The experiment was repeated for each of the microcapsules with different shell thicknesses. The weight loss of each sample, caused by CO_2 gas release, was automatically recorded every 5 s by a computer connected to the balance. The weight loss curve of 0.5 g of crude $CaCO_3$ in the same acid solution was also recorded as a reference.

Thermal conversion of the inner guest materials

$CaCO_3$ containing zeolite microcapsules were calcined at 850 °C for 1 h in air at a heating rate of 5 °C min^{-1} to convert $CaCO_3$ into CaO, and then the hygroscopic CaO cores were transformed into $Ca(OH)_2$ by reacting with water molecules from the atmosphere. Fe_2O_3 containing zeolite microcapsules were obtained by calcining the zeolite microcapsules with $Fe_3(SO_4)_2(OH)_5 \cdot 2H_2O$ cores at 900 °C for 1 h in air at a heating rate of 5 °C min^{-1}.

Acknowledgements

This work is financially supported by the NSFC (20273016, 20233030, 20303003, 20325313), the SNPC (0249nm028, 03DJ14004) and the Major State Basic Research Development Program (2000077500, 2003CB615807).

References

1 J. A. Thomas, L. Seton, R. J. Davey and C. E. DeWolf, *Chem. Commun.*, 2002, 1072.
2 (*a*) H. Huang, E. E. Remsen, T. Kowalewski and K. L. Wooley, *J. Am. Chem. Soc.*, 1999, **121**, 3805; (*b*) F. Caruso, D. Trau, H. Möhwald and R. Renneberg, *Langmuir*, 2000, **16**, 1485; (*c*) L. Dähne, S. Leporatti, E. Donath and H. Möhwald, *J. Am. Chem. Soc.*, 2001, **123**, 5431; (*d*) M. Sauer, D. Streich and W. Meier, *Adv. Mater.*, 2001, **13**, 1649; (*e*) L. S. Zha, Y. Zhang, W. L. Yang and S. K. Fu, *Adv. Mater.*, 2002, **14**, 1090; (*f*) C. Y. Gao, S. Leporatti, S. Moya, E. Donath and H. Möhwald, *Chem.-Eur. J.*, 2003, **9**, 915.
3 (*a*) D. L. Wilcox and M. Berg, *Mater. Res. Soc. Symp. Proc.*, 1995, **372**, 3; (*b*) P. Tartaj, T. González-Carreño and C. J. Serna, *Adv. Mater.*, 2001, **13**, 1620; (*c*) M. Kim, K. Sohn, H. B. Na and T. Hyeon, *Nano Lett.*, 2002, **2**, 1383.
4 (*a*) R. Arshady, *Polym. Eng. Sci.*, 1990, **30**, 915; (*b*) W. Frere, L. Danicher and P. Gramain, *Eur. Polym. J.*, 1998, **34**, 193; (*c*) R. S. Winder, J. J. Wheeler, N. Conder, I. S. Otvos, R. Nevill and L. Duan, *Biocontrol. Sci. Technol.*, 2003, **13**, 155.
5 C. Thies, *Microencapsulation Encycopaedia of Polymer Science and Engineering*, Wiley, New York-Chichester, 2nd edn., 1987, pp. 724–745.
6 (*a*) K. H. Rhodes, S. A. Davis, F. Caruso, B. J. Zhang and S. Mann, *Chem. Mater.*, 2000, **12**, 2832; (*b*) X. D. Wang, W. L. Yang, Y. Tang, Y. J. Wang, S. K. Fu and Z. Gao, *Chem. Commun.*, 2000, 2161; (*c*) V. Valtchev, *Chem. Mater.*, 2002, **14**, 4371; (*d*) S. P. Naik, A. S. T. Chiang, R. W. Thompson and F. C. Huang, *Chem. Mater.*, 2003, **15**, 787.
7 (*a*) A. G. Dong, Y. J. Wang, Y. Tang, N. Ren, Y. H. Zhang and Z. Gao, *Chem. Mater.*, 2002, **14**, 3217; (*b*) A. G. Dong, Y. J. Wang, D. J. Wang, W. L. Yang, Y. H. Zhang, N. Ren, Z. Gao and Y. Tang, *Microporous Mesoporous Mater.*, 2003, **64**, 69.
8 N. Nishiyama, M. Miyamoto, Y. Egashira and K. Ueyama, *Chem. Commun.*, 2001, **1746**.
9 T. Nakai and H. Nakamaru, in *Industrial Crystallization '78*, eds. E. J. Jongde and S. J. Jancic, North-Holland, New York, 1979, pp. 75–79.
10 A. E. Persson, B. J. Schoeman, J. Sterte and J. E. Otterstedt, *Zeolites*, 1994, **14**, 557.
11 M. Lassinantti, F. Jareman, J. Hedlund, D. Creaser and J. Sterte, *Catal. Today*, 2001, **67**, 109.